

- [3] L. Devroye and T. J. Wagner, "Distribution-free consistency results in nonparametric discrimination and regression function estimation," *Ann. Statist.*, vol. 8, pp. 231-239, 1980.
- [4] L. Devroye and G. L. Wise, "Consistency of a recursive nearest neighbor regression function estimate," *J. Multivariate Anal.*, vol. 10, pp. 539-550, 1980.
- [5] L. Gordon and R. A. Olshen, "Asymptotically efficient solutions to the classification problem," *Ann. Statist.*, vol. 6, pp. 515-533, 1978.
- [6] L. Gyorfi, "Recent results on nonparametric regression function estimate and multiple classification," in *Problems of Control and Information Theory*, 1981.
- [7] R. A. Olshen, "Comment on a paper by C. J. Stone," *Ann. Statist.*, vol. 5, pp. 632-633, 1977.
- [8] C. Spiegelman and J. Sacks, "Consistent window estimation in nonparametric regression," *Ann. Statist.*, vol. 8, pp. 240-246, 1980.
- [9] C. J. Stone, "Consistent nonparametric regression," *Ann. Statist.*, vol. 8, pp. 595-645, 1977.



Luc Devroye was born in Tienen, Belgium, on August 6, 1948. He received the Ph.D. degree from the University of Texas, Austin, in 1976.

In 1977 he became an Assistant Professor at the School of Computer Science, McGill University, Montreal, P.Q., Canada. He is interested in various applications of probability theory and mathematical statistics such as nonparametric estimation, probabilistic algorithms, the computer generation of random numbers, and the strong convergence of random processes.

A Model for Radar Images and Its Application to Adaptive Digital Filtering of Multiplicative Noise

VICTOR S. FROST, STUDENT MEMBER, IEEE, JOSEPHINE ABBOTT STILES, STUDENT MEMBER, IEEE,
K. S. SHANMUGAN, SENIOR MEMBER, IEEE, AND JULIAN C. HOLTZMAN, MEMBER, IEEE

Abstract—Standard image processing techniques which are used to enhance noncoherent optically produced images are not applicable to radar images due to the coherent nature of the radar imaging process. A model for the radar imaging process is derived in this paper and a method for smoothing noisy radar images is also presented.

The imaging model shows that the radar image is corrupted by multiplicative noise. The model leads to the functional form of an optimum (minimum MSE) filter for smoothing radar images. By using locally estimated parameter values the filter is made adaptive so that it provides minimum MSE estimates inside homogeneous areas of an image while preserving the edge structure. It is shown that the filter can be easily implemented in the spatial domain and is computationally efficient. The performance of the adaptive filter is compared (qualitatively and quantitatively) with several standard filters using real and simulated radar images.

Index Terms—Adaptive filtering, image enhancement, minimum mean square error (MMSE), multiplicative noise, radar image modeling, radar image processing, speckle reduction, synthetic aperture radar (SAR).

I. INTRODUCTION

ALARGE number of image restoration and enhancement techniques have been proposed in recent years for removing a variety of degradations in recorded images of objects and scenes. These degradations result from the nonideal nature of practical imaging systems. The design of optimum

Manuscript received September 8, 1980; revised September 21, 1981. This work was supported by the California Institute of Technology President's Fund, NASA under Contract NAS 7-100, and the U.S. Army Research Office under Contract DAAG29-77-G-0075.

The authors are with the Remote Sensing Laboratory, Center for Research, Inc., University of Kansas, Lawrence, KS 66045.

image restoration and enhancement techniques requires a mathematical model of the imaging process. This paper presents a model for the noise in radar images and uses the model to develop an adaptive algorithm to smooth noisy nonstationary images.

Imaging radars, specifically the synthetic aperture radar (SAR), are beginning to make use of the digital techniques, and digitally correlated SAR images are now becoming available. However, optimum techniques for digitally processing radar images are not fully developed due to a lack of understanding of the properties of radar images from a digital image processing perspective. Thus, there is an important need for developing statistical models for radar noise and for using them in deriving appropriate algorithms for processing radar images.

This paper presents a model and a model-based image enhancement technique which is specifically designed for active microwave sensors utilizing coherent imaging techniques. The model portrays the observed radar image as corrupted by multiplicative-convolved noise. That is, the desired information, the terrain backscatter, is multiplied by a stationary random process which represents the effects of coherent fading [1]-[3]. The product signal is then processed (convolved) with the point spread function of the radar system to produce the observed image.

This model can be applied to the design of digital image enhancement algorithms through several approaches. The procedure used here was to develop a minimum mean square error (MMSE) filter to estimate the terrain backscatter from the

image data. The design of an MMSE filter is predicated on the assumption of stationarity of both the signal and the noise, but the image is nonstationary on a global basis. For radar the noise can be modeled as being stationary but the signal is nonstationary since the mean backscatter changes with the type of target being sensed. Therefore, it is necessary to adapt the filter to changes in local properties of the terrain backscatter. Analysis of the system model shows that only the local observed mean and standard deviation are required to properly adapt the filter so that it produces the MMSE estimates inside homogeneous (stationary) areas while preserving edge structure.

The performance of the adaptive filter is compared with other filters using simulated [4] and actual Seasat-SAR digital imagery. A number of qualitative and quantitative performance measures are used for comparison and the results show that the adaptive filter performs better than many of the commonly used filters.

Even though this adaptive enhancement technique has been developed and evaluated for radar, it is applicable for other types of images. Obviously, it is applicable for coherent speckle reduction in general, as the noise processes are similar for all coherent sensors [2]. Further, the approach described in this paper can be used for developing adaptive filtering algorithms for other applications in which the image is corrupted by multiplicative noise. Because of its simple spatial domain implementation the adaptive filtering algorithms provide an alternative to homomorphic filtering [5].

The contents of the paper are organized as follows. Section II contains the background of the modeling and filtering problem. In Section III the model for noise in radar images is developed from a digital image processing perspective. The MMSE filter is derived in Section IV and the criteria for the adaptation of the filter based on local statistics is discussed. The utility of this adaptive processing algorithm is evaluated in Section V using both real and simulated radar images. It is shown qualitatively and quantitatively that the adaptive filter improves the ability of both human and machine interpreters to extract pertinent information from radar images. Recommendations and conclusions are presented in Section VI.

II. BACKGROUND

A SAR image is constructed by processing the two-dimensional complex waveform received by the sensor (when stored photographically these raw data are called the signal film). This processing is performed either by a coherent optical system [6] or a digital computer [7]. The output of this processing is a complex image whose properties are well known [8]. For a region within the sensed terrain which is homogeneous and which is classified as a distributed target (i.e., it is composed of a single target class, e.g., corn or trees, and contains many scatters no one of which predominates), the complex image is statistically characterized by a narrow-band white Gaussian random process.

The standard technique for enhancing SAR images is to use noncoherent integration [11]-[13]. Enhancement implies increasing the signal-to-noise ratio at the expense of spatial resolution [14], [15]. Most SAR systems use frequency diversity,

i.e., nonoverlapping subareas of the spectrum of the complex image are used to form N independent images. Continuous scanning of the spectrum is also used [13], [17], [18]. The net effect is to reduce the bandwidth (degrade the resolution) while improving the signal-to-noise ratio S/N . Several studies [12], [14], [15] have shown the advantages of noncoherent processing for the interpretation of SAR imagery. However, there are several disadvantages to this approach: 1) the technique is spatially invariant and thus does not account for the nonstationarity of the signal; 2) the technique was developed for coherent optical processing and thus it is easily implemented with such a processor but is not necessarily optimal for digital processing. A technique is thus needed to take full advantage of digital image processing for radar. Several different existing approaches have been considered.

Linear spatially invariant filters have been used extensively in digital image processing [19]-[21]. These techniques are primarily designed for recovering "ideal" images distorted by linear spatially invariant operations in the presence of additive noise [20]. The nonstationarity of the ideal images is not accounted for in most of these techniques and thus these methods tend to blur edges. Furthermore, these techniques are not suited to radar imagery because of the multiplicative nature of the noise.

Homomorphic filtering [5] is applicable to images corrupted by multiplicative noise. Homomorphic filtering refers to a technique of preprocessing the observed image to transform nonadditive noise into additive noise using some nonlinear memoryless operator. Then standard techniques are applied for additive noise reduction. The enhanced data are then formed by applying the inverse nonlinear operator. For multiplicative noise logarithmic and exponential operators are required. The model for radar images (which will be derived in the next section) represents the observed data as being multiplicative noise operated on by a linear system, or viewed from another perspective, each output pixel (picture element) is a weighted sum (convolution) of a product. A logarithmic operation will not properly separate the signal from the noise for this case. A possible solution for this would be to deconvolve [20] the observed data to remove the effects of the linear system and then to apply homomorphic filtering. Unfortunately, the performance of deconvolution techniques degrades rapidly as the signal-to-noise (S/N) ratio decreases [20] (especially if there are zeros in the system function). Radar images already have a low S/N ratio, and hence the inverse filtering does not produce images of acceptable quality.

There have been some other approaches to image processing for multiplicative noise. Most of these have been concerned with image restoration in the presence of film-grain noise. Multiplicative noise is treated by Walkup and Choens [22] where a grain noise model is presented and a Wiener filter is designed for this particular model. As in the case of linear filtering, the nonstationarity of the signal characteristics was not incorporated. Wiener filtering for multiplicative noise was also treated by Kondo *et al.* [23]. A system model similar to the one developed here for radar noise is presented for film granularity. Again, a Wiener filter is derived and the ideal signal is assumed to be stationary. Naderi and Sawchuk [24] follow

the same basic approach of the previous papers, i.e., a model for film grain noise is presented and a discrete Wiener filter is developed. Here the nonstationarity of the signal is treated and an adaptive technique is presented. This adaptive filter assumes a constant form for the variance and second-order properties of the ideal image and the filter only changes relative to the local mean. Thus, the nonstationary effects as manifested by variations in the local mean are accounted for, while all second-order properties are assumed stationary. In addition, the approach of Naderi and Sawchuk requires extensive computations. Each of these techniques treats multiplicative noise; however, none were seen as being directly applicable to radar image data even though they do provide some insight as to the appropriate direction to pursue.

Nonlinear and adaptive image enhancement techniques have been developed in a wide variety of forms. A simple nonlinear operator is the median filter [19]. This filter replaces each pixel value with the median of its neighbors. The median filter is heuristic and is not based on any specific image model. The performance of this operator was evaluated with respect to radar image processing and the results are presented in Section V of this paper. Other adaptive algorithms have been proposed, many of which are derived using a Kalman filter approach. Chen [25] presented one such algorithm. The major disadvantages of these techniques are computational inefficiency and the assumption of additive noise.

A heuristic adaptive filter is proposed by Panda [26]. This algorithm is not applicable to radar images because of its additive noise assumption and the criterion for filter adaptation is not suitable. However, it is interesting to note that the basic filter shape is very similar to the one developed here. Recently, Lee [27] suggested the use of local statistics to adapt image enhancement algorithms for both additive and multiplicative noise.

III. A MODEL FOR PROCESSING DIGITAL RADAR IMAGES

The purpose of this section is to present a statistical description for radar images which is suitable for use in the development of digital image enhancement and feature extraction algorithms. Many sophisticated models [6] have been developed for SAR systems; however, these were derived for system design and not for image processing.

As previously discussed, the complex radar image of a homogeneous area can be represented by a narrow-band Gaussian process. The first-order statistics of the received power of such a signal are known to have an exponential probability density function (pdf) [1]. If noncoherent averaging is performed, then the pdf for the power follows a gamma distribution [2], i.e.,

$$f_{P_r}(P_r(x_0, y_0)) = \frac{P_r^{N-1}(x_0, y_0) \exp\left[-\frac{P_r(x_0, y_0)}{\bar{P}_r/N}\right]}{(N-1)! \left(\frac{\bar{P}_r}{N}\right)^N} \quad (1)$$

where

$P_r(x_0, y_0)$ = observed power at position x_0, y_0

$\bar{P}_r = E[P_r(x_0, y_0)]$ = the expected value of the observed power at position x_0, y_0

N = number of independent images averaged by the sensor.

The observed power can be rewritten as [28], [29]

$$P_r(x_0, y_0) = \frac{\bar{P}_r n(x_0, y_0)}{2N} \quad (2)$$

where the fluctuations of $P_r(x_0, y_0)$ are governed by the random variable $n(x_0, y_0)$. This random variable represents the fading variations. The pdf of $n(x_0, y_0)$ is given by

$$f_n(n(x_0, y_0)) = \frac{n^{N-1}(x_0, y_0) \exp\left[-\frac{n(x_0, y_0)}{2}\right]}{(N-1)! 2^N} \quad (3)$$

which is a standard chi-square distribution. Equation (2) separates the observed power into: 1) a signal independent fading component $n(x_0, y_0)$ which is stationary, non-Gaussian with nonzero mean, and 2) a mean value component. That is, the moments of $n(x_0, y_0)$ are solely a function of N which is a system parameter, while the moments of $P_r(x_0, y_0)$ are dependent upon the desired signal parameter \bar{P}_r .

Equation (2) can be generalized to represent the first-order properties of the observed power by allowing x_0, y_0 to become variables, i.e.,

$$P_r(x, y) = \frac{\bar{P}_r(x, y) n(x, y)}{2N} \quad (4)$$

$\bar{P}_r(x, y)$ represents the expected value of the observed power as a function of position. If stationarity is assumed, then $\bar{P}_r(x, y)$, which is defined as an expected value, is a constant for an ensemble of similar homogeneous areas. $\bar{P}_r(x, y)$ is proportional to the terrain backscatter coefficient σ^0 for that class of targets [30].

However, actual measurements of a single area (i.e., one sample function) will exhibit random variation in σ^0 . Real terrain scenes are composed of many homogeneous areas each having different average backscatter such that field boundaries exist. It is reasonable to model \bar{P}_r as a slowly varying function of position and to define a new random process $r(x, y)$, which is actually the desired image, to represent these variations. The observed power can thus be written as

$$P_r(x, y) = r(x, y) \cdot n(x, y). \quad (5)$$

Clearly, the random process $P_r(x, y)$ is not stationary because its expected value is a function of position. However, it is reasonable to assume that $n(x, y)$ is stationary and $r(x, y)$ is stationary in homogeneous areas.¹

The recorded radar image $I(x, y)$ is not simply proportional to the observed power on a point-by-point basis. There are several components of a SAR system, e.g., the antenna, receiver, and correlator which introduce a spatial correlation.

¹The above discussion assumes a power display format; however, this model is applicable for other display formats or multiplicative noise models. Only the form of (3) is changed.

These components can be represented by a single linear spatially invariant transfer function [6]. Therefore, the recorded radar image is modeled by

$$I(x, y) = [r(x, y) \cdot n(x, y)] * h(x, y) \quad (6)$$

where $h(x, y)$ is the system impulse response and $*$ denotes convolution. Equation (6) is the model of a SAR image suitable for use in developing digital processing algorithms. The estimation technique presented next attempts to remove the fading noise (the dominant source of randomness in radar images) and generate an estimate of the "ideal image" $r(x, y)$ from the observed image $I(x, y)$.

IV. DEVELOPMENT OF AN ENHANCEMENT TECHNIQUE BASED ON THE IMAGE MODEL

The image enhancement technique to be developed in this section is based on the model described in the previous section. The approach that was followed was to first derive the functional form of the minimum mean square error (MMSE) filter to estimate $r(x, y)$ from $I(x, y)$ under the assumptions of stationary image data. The nonstationary aspects of real SAR data are then incorporated by identifying the important filter parameters which vary with position, and by determining a method for estimating the parameter values from the observed image. The result of this analysis is an adaptive filter which is computationally efficient, provides the MMSE estimate in homogeneous areas, and tends to preserve the edge structure of the image.

The impulse response $m(t)$ and the transfer function $M(f)$ of the minimum mean square error (MMSE) filter that provides an estimate of $r(t)$ from $I(t)$ is obtained by minimizing the mean square error ϵ^2 given by

$$\epsilon^2 = E[(r(t) - I(t) * m(t))^2] \quad (7)$$

where $t = (x, y)$ is the spatial coordinate. The MMSE solution [31] leads to a transfer function

$$M(f) = \begin{cases} \left[\frac{\bar{n}S_r(f)}{S_r(f) * S_n(f)} \right] \frac{1}{H^*(f)} & \text{for } f \neq 0 \\ \frac{1}{\bar{n}} & \text{for } f = 0 \end{cases} \quad (8)$$

where $\bar{n} = E\{n(t)\}$ and $f = (f_x, f_y)$ is the spatial frequency coordinate. $S_r(f)$ and $S_n(f)$ are the power spectral densities of the terrain reflectivity and the noise process, respectively. The filter given in (8) is valid for processing image data within homogeneous areas inside of which $r(t)$ can be modeled as a stationary random process. In (8) $H^*(f)$ is the complex conjugate of the transfer function of the system which is not data dependent, and hence can be assumed constant over some finite bandwidth. The data dependent part of the filter is $M'(f)$, which can be written as

$$M'(f) = \frac{\bar{n}S_r(f)}{S_r(f) * S_n(f)}. \quad (9)$$

The standard model for $r(t)$ is an autoregressive process with an autocorrelation function $R_r(\tau)$ and a two-sided power spectral density $S_r(f)$ [32] of the form

$$R_r(\tau) = \sigma_r^2 e^{-a|\tau|} + \bar{r}^2 \quad (10a)$$

$$S_r(f) = \frac{2\sigma_r^2 a}{a^2 + 4\pi^2 f^2} + \bar{r}^2 \delta(f) \quad (10b)$$

where the parameters σ_r^2 , \bar{r}^2 , and "a" have different values for different terrain categories. The model for the multiplicative white noise is

$$R_n(\tau) = \sigma_n^2 \delta(\tau) + \bar{n}^2 \quad (11a)$$

$$S_n(f) = \sigma_n^2 + \bar{n}^2 \delta(f) \quad (11b)$$

where the parameters σ_n^2 and \bar{n}^2 are sensor dependent but are not scene dependent. Substituting the power spectral densities of $r(t)$ and $n(t)$ into (9), it can be shown that the impulse response of the filter is given by [33]

$$m'(t) = K_1 \alpha e^{-\alpha|t|} \quad (12)$$

with

$$\alpha = \sqrt{2a \left[\frac{\bar{n}}{\sigma_n} \right]^2 \cdot \left[\frac{1}{1 + \left(\frac{\bar{r}}{\sigma_r} \right)^2} \right] + a} \quad (13)$$

where K_1 is a normalizing constant.

The MMSE filter described by (12) has some interesting properties. We have tacitly assumed that both $r(t)$ and $n(t)$ are wide-sense stationary random processes. This assumption regarding $n(t)$ is valid over an entire radar image because both \bar{n} and σ_n^2 are functions of system parameters which can be assumed to be constant. But $r(t)$ is stationary only in individual homogeneous regions, and thus the filter is theoretically applicable in only those areas. However, if α is varied continuously (adapted) with respect to scene conditions, then the filter will provide the MMSE estimate in all homogeneous areas.

To evaluate its performance at edges consider two homogeneous (stationary) areas A_1 and A_2 with $\bar{r}_1 = \bar{r}_2$ and $\sigma_{r_1}^2 > \sigma_{r_2}^2$, then from (13) we find that

$$\alpha_1 > \alpha_2. \quad (14)$$

This result indicates that the impulse response of the MMSE filter for A_1 is narrower than the filter for A_2 . If $r(t)$ has a large variance, then a wide impulse response would excessively average the desired variation in backscatter. Thus, for areas with σ_r^2 large the impulse response of the filter should be narrow.

Next consider an area A_3 which contains a boundary between two stationary areas A_1, A_2 . First, note that A_3 is not a stationary area so theoretically this MMSE filter does not provide the minimum mean square estimate. However, the presence of an edge will result in a large variance for $r(t)$ in A_3 . That is,

$$\sigma_{r_3}^2 > \sigma_{r_1}^2 \quad (15)$$

and

$$\sigma_{r_3}^2 > \sigma_{r_2}^2. \quad (16)$$

So for an area encompassing an edge, the MMSE filter will average less and therefore preserve edge structure.

If α is estimated from the observed data within some local neighborhood of each position (x, y) , the MMSE filter could then be adapted to local changes. This enhancement technique would then exhibit two very important characteristics. First, it provides the MMSE estimate of $r(t)$ in homogeneous areas. Second, it tends to preserve edge structure.

The decay constant α is a function of all three signal parameters σ_r^2 , \bar{r} , and "a." As consecutive homogeneous areas are examined, σ_r^2 and \bar{r} will change significantly but "a" will vary only by a small amount. Thus, for the purposes of adapting the filter σ_r^2 and \bar{r} can be assumed to vary while "a" can be treated as a constant. It is left to determine what local properties of the observed image can be used to estimate $(\bar{r}/\sigma_r)^2$, and thus to determine how α is to be varied.

The ratio of the observed image variance to the square of the mean will be shown to provide the required information to properly adapt the filter. The expected value of the observed image in a homogeneous area is given by

$$\bar{I} = E[I(t)] = \bar{n}\bar{r}H(0). \quad (17)$$

$H(0)$ is assumed to be unity. The variance of the observed image is defined as

$$\sigma_I^2 = E[I^2(t)] - \bar{I}^2. \quad (18)$$

The mean square $E[I^2(t)]$ can be found by

$$E[I^2(t)] = \int_{-\infty}^{\infty} S_I(f) df \quad (19)$$

where $S_I(f)$ is the power spectral density of the observed image. From (6) it can be shown that

$$S_I(f) = S_r(f) * S_n(f) |H(f)|^2. \quad (20)$$

So

$$\begin{aligned} E[I^2(t)] &= \int_{-\infty}^{\infty} |H(f)|^2 \int_{-\infty}^{\infty} S_r(z) S_n(z-f) dz df \\ &= \int_{-\infty}^{\infty} S_r(z) \int_{-\infty}^{\infty} |H(f)|^2 S_n(z-f) df dz. \end{aligned} \quad (21)$$

Substituting the specific form of $S_n(f)$ into (21) and performing the integration the mean square value becomes

$$E[I^2(t)] = k_h \sigma_n^2 \int_{-\infty}^{\infty} S_r(z) dz + \bar{n}^2 \int_{-\infty}^{\infty} S_r(z) |H(z)|^2 dz$$

where

$$k_h = \int_{-\infty}^{\infty} |H(f)|^2 df. \quad (22)$$

The dependence on the system transfer function $H(f)$ can be removed from the rightmost term of (22) because $r(t)$ has been assumed to be a slowly varying function of position. The effect of $S_r(f)$ thus predominates, and using the following definition:

$$\int_{-\infty}^{\infty} S_r(z) dz = \sigma_r^2 + \bar{r}^2 \quad (23)$$

the desired ratio is found to be

$$\frac{\sigma_I^2}{\bar{I}^2} = \frac{\sigma_r^2}{\bar{r}^2} k_s + k_b$$

where

$$\begin{aligned} k_s &= \frac{k_h \sigma_n^2}{\bar{n}^2} + 1 \\ k_b &= \frac{k_h \sigma_n^2}{\bar{n}^2}. \end{aligned} \quad (24)$$

The importance of (24) is that it shows that to estimate the changes in σ_r^2/\bar{r}^2 and thus α , only the observed mean and variance need to be found, i.e., to properly adapt the filter the local sample mean and variance are used. The decay constant is now written as

$$\alpha^2 \propto \sigma_I^2 / \bar{I}^2. \quad (25)$$

To process the image at location (x_0, y_0) , the parameters \bar{I}^2 and σ_I^2 are estimated using data from a local neighborhood (say a 5×5 window) centered at (x_0, y_0) . The adaptive filter performs a weighted average of data in the neighborhood of (x_0, y_0) , the weights being determined from the local statistics of the data using (25) and (12). Note that the window used to gather the local statistics can be larger than the one used to perform the filtering. The results presented in this paper were generated by continuously adapting α to changes in the local statistics. These statistics were gathered using a 5×5 window; also, the filter operated on a 5×5 neighborhood.

The idea of using local statistics as a basis for spatially varying image enhancement is not new [27] and its advantages, e.g., computational efficiency, are well known. However, the technique presented here has a firm theoretical basis and it exhibits several additional beneficial properties, i.e., it provides the MMSE estimate in homogeneous areas and preserves edge structure. Even though this algorithm has been developed specifically for radar images, the technique is generally applicable to images corrupted by multiplicative noise and should provide an alternative to homomorphic filtering because of its simple implementation.

V. RESULTS

Radar images processed by the MMSE adaptive filter are presented and evaluated in this section. This assessment is performed in two ways. First, a qualitative evaluation is conducted using real sensor images (in this case digitally correlated Seasat-A SAR data). Even though the adaptive filter was developed to minimize the mean square error which does not necessarily correlate to any improvement in interpretability (either human or machine [40]), these results demonstrate that the algorithm does in fact enhance the utility of radar images for important applications, e.g., target discrimination, geologic analysis, and agricultural assessment. For quantitative evaluations of the image enhancement algorithm we use an edge figure of merit proposed by Pratt [19].

A. Qualitative Evaluation of the Adaptive Filter Using Digital Seasat-A SAR Imagery

The adaptive filter derived for multiplicative noise was applied to several digitally processed synthetic aperture radar images which were provided by the Jet Propulsion Laboratory. Seasat-A SAR images, some processed to signal-to-noise ($S/N = 1$, 50 m resolution and some processed for $S/N = 14.6$, 25 m resolution, were operated on by the adaptive filter as well as with several standard image noise reduction techniques well known in the digital image processing field. These filters were: 1) the median filter, 2) a 3×3 box filter (uniformly weighted averaging over a 3×3 window), and 3) a 5×5 box filter (uniformly weighted averaging over a 5×5 window).

The first digital SAR image processed by the noise reduction filters is a scene containing the target responses of nine (non-equal cross section) corner reflectors used to represent point targets for the sensor at Goldstone, California (see Goldfinger [34] for a complete description of the test site). Fig. 1 contains the original image ($S/N = 1$, 50 m resolution) and four filtered versions. The digital display from which these scenes were photographed has a 512×512 pixel, 256 gray level format (each square pixel represents a 36×36 m area). The original image has a poor signal-to-noise ratio, which makes it difficult to unambiguously locate the corner reflectors and to describe the surrounding terrain. The 3×3 and the 5×5 box filters smooth the image without regard to neighborhood statistics, thus spreading the point target returns, although these filters might facilitate gross scale structural analysis of the scene. These filters perform a simplistic tradeoff of resolution for averaging. The median filter produces a visible signal-to-noise improvement, and it does not blur the image as do the box filters. However, the response to the point targets becomes much dimmer as the high intensity pixel values are replaced by their respective median values. Since these target returns are of interest to us, the median filter's performance is inferior to the box filter's. The adaptive filter preserves the small spatial extent of the point targets and the brightened foreslopes of the terrain, and averages as does a box filter in regions which are homogeneous.

Focusing our attention next on the region containing the point targets, we compare the responses of the filters in detail. Fig. 2 is the composite of photographs of the point targets taken from an isometric display. The original image, with its various intensities displayed as "heights," demonstrates the extreme noisiness of the SAR image. The point target retention characteristics of the adaptive filter are easily seen. Eight of the nine point targets are detectable at this level of magnification.

A primarily agricultural Seasat-A scene ($S/N = 14.6$, 25 m resolution, 17 m pixel spacing) is shown in Fig. 3 along with an adaptively filtered version of the site. The effects of averaging in extensive homogeneous regions are visible, and field boundaries are shown to be well preserved in the adaptively filtered version. A third Seasat-A SAR image which contains both agricultural elements and geologically interesting structures was also adaptively processed. Fig. 4 shows a location in Tennessee through which the Holston River flows (in the

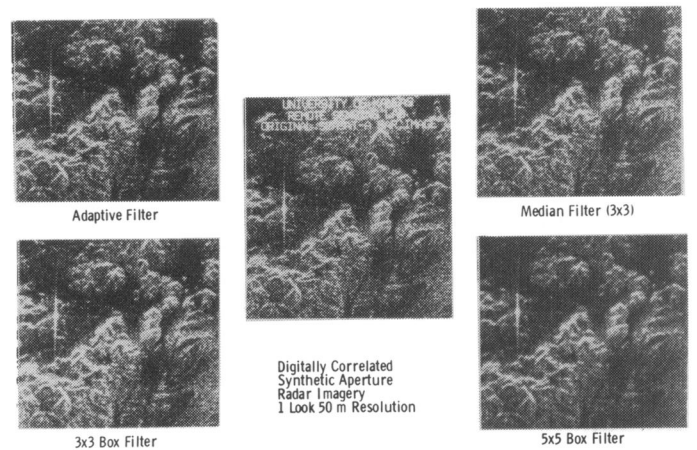


Fig. 1. Comparison of processing algorithms on Seasat-A SAR imagery.

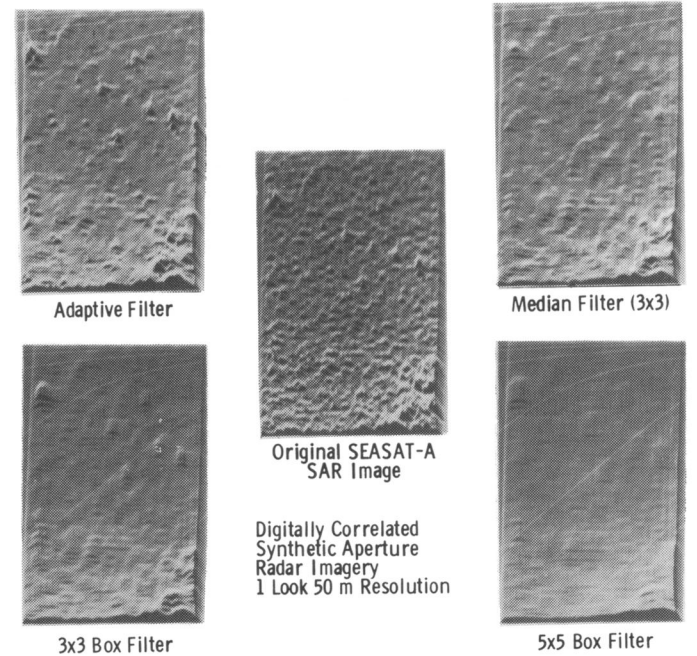


Fig. 2. Comparison of processing algorithms on Seasat-A SAR imagery (isometric display).

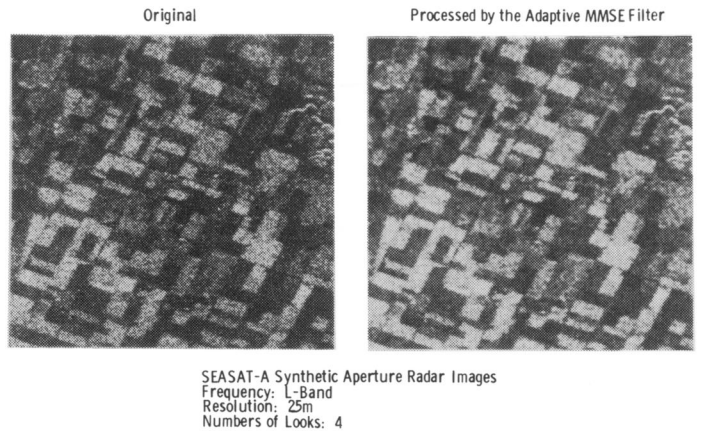


Fig. 3. Example of adaptive filter on agricultural features.

lower left-hand corner of the photographs). The primary improvements noticed in this comparison study are the more clearly defined field boundaries near the bend and greater definition of the ridges between the foreslopes and backslopes

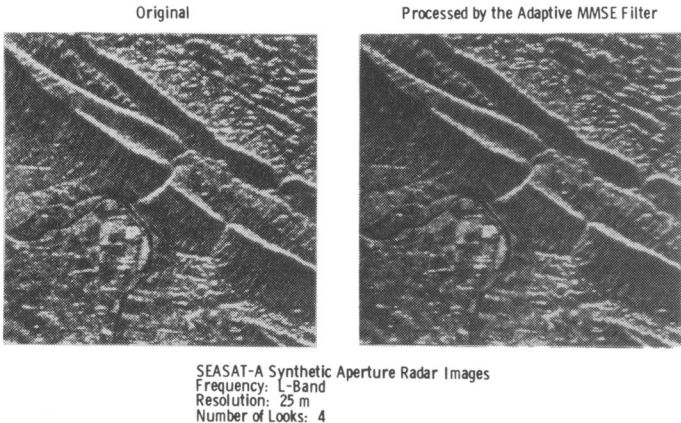


Fig. 4. Example of adaptive filter on geologic and agricultural features.

of the terrain above the bend. The adaptive processing of radar images of this type does facilitate a more rapid analysis for geologic and hydrologic purposes because strong linear features are emphasized as Fig. 4 illustrates [41].

B. Quantitative Evaluation of the Adaptive Filter Using an Edge Map Quality Criterion

In this section the performance of the filters are quantitatively compared using edge maps generated from enhanced images. This approach was selected because: 1) a quantitative figure of merit for edge maps has recently been reported [19], [35], and 2) edge maps are used as an intermediate step in many image segmentation and classification algorithms. Five processing algorithms were evaluated: the adaptive, median, 3×3 box and 5×5 box filters, and noncoherent integration.

To evaluate these processing algorithms the following procedure was used: 1) produce the input images, 2) apply the enhancement operators, 3) apply a Robert's gradient operator [19] to each enhanced image, 4) threshold the gradient images, and 5) apply the figure of merit.

An edge map is a binary image where a "1" at location (i, j) indicates that the pixel at (i, j) is on an edge, while a "0" indicates the absence of an edge. The edge figure of merit used here is the one proposed by Pratt [19]. Define two congruent images I_I and I_A , representing ideal and actual edge maps of a single step edge of height h . The ideal edge map contains N_I edge pixels, while the actual edge map contains N_A . Further, define d as the perpendicular distance from an actual edge pixel to the ideal edge. The edge figure of merit is then defined by

$$R = \frac{1}{\max(N_A, N_I)} \sum_{i=1}^{N_A} \frac{1}{1 + \beta d^2}$$

where

β = scaling constant.

The scaling constant β allows the user to weight the penalty for offset localized edges (for this experiment $\beta = \frac{1}{9}$, following Pratt [19]). Further details concerning R are found in [35].

Input images for this experiment were generated using a radar image simulation package available at the Remote Sensing Laboratory [4]. Six simulated images were produced for three different edge step heights of 3, 6, and 9 dB (i.e., the

mean radar backscatter in dB for each side of the edge differed by the given amount) and two signal-to-noise ratios 1 and 14.6. The resolution and dynamic range were set to approximate that of the Seasat-A SAR, i.e., a resolution of 25 m with a pixel spacing of 17 m. The image size was 145×145 pixels.

Each of the images described above was filtered first and then further processed by a Robert's gradient. The selection of the threshold greatly affects the nature of the edge maps. An optimum threshold (i.e., the threshold which maximizes R) was found experimentally for each processed scene assuming the 3 dB edge is a worst case. That is, for all images (either $S/N = 1$ or $S/N = 14.6$) processed by a particular algorithm, a single optimum threshold was applied to the 3, 6, and 9 dB images. This treats the 3, 6, and 9 dB edges as having occurred in the same image.

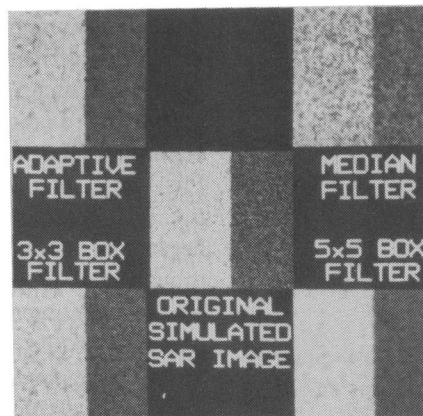
The edge quality results are summarized in Table I. There are several interesting observations to be made from these data. First, note for the $S/N = 1$ case that R decreased slightly from the 3 dB edge to the 6 dB edge in several cases. This occurred because of the basic multiplicative nature of radar data. Even though there is a greater edge contrast, the edge quality (based on this experiment) does not improve because the variance on one side of the edge has also increased. This is true until enough averaging has been performed, e.g., $S/N = 1, 5 \times 5$ box and adaptive filter, and all the $S/N = 14.6$ images except the original image.

Another important observation is that the Robert's gradient/global threshold technique does not provide adequate edge maps for any of the $S/N = 1$ images and only the adaptive filter produces adequate edge maps for the $S/N = 14.6$ data. Further, note that the adaptive filter clearly provides superior edge maps with respect to the original 3×3 box, and median filter for both the $S/N = 1$ and $S/N = 14.6$ cases. The 5×5 box filter does provide comparable results except for the $S/N = 14.6$, 3 dB case, where the adaptive filter produces a figure of merit which is 20 percent higher. This last case is significant because it shows that the adaptive filter is less sensitive to the edge height as expected from its adaptive nature. Thus, the adaptive technique performs well on low contrast edges; these are the ones where the most enhancement is needed. Even though the 5×5 box filter performs as well as the adaptive filter when there is sufficient edge contrast, the adaptive technique is still seen as superior because of resolution considerations. Also, the adaptive filter operating on the $S/N = 1$ images produced better edge maps than were produced noncoherently averaging the $S/N = 1$ image to a $S/N = 14.6$, i.e., using this criterion the adaptive filter is slightly better than noncoherent averaging, especially for the larger edge contrasts. Combining these results with the response of each technique to the corner reflectors and a S/N versus bandwidth analysis [33], the adaptive filter does provide superior results.

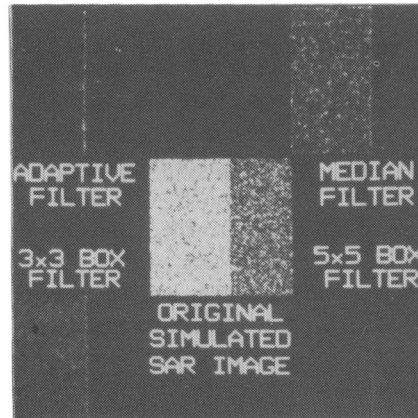
Results are shown for the $S/N = 14.6$ and 6 dB edge height in Fig. 5(a)-(c). The original simulated image and the four enhanced images are given in Fig. 5(a). The output of the Robert's gradient are shown in Fig. 5(b). These gradient images demonstrate an important statistical property of radar images, i.e., any form of high pass filtering on a radar image generates a noisier image with radar "like" properties, and thus

TABLE I
RESULTS OF EDGE FIGURE OF MERIT STUDY. FIGURE OF MERIT IN
PERCENTAGE VERSUS PROCESSING ALGORITHM

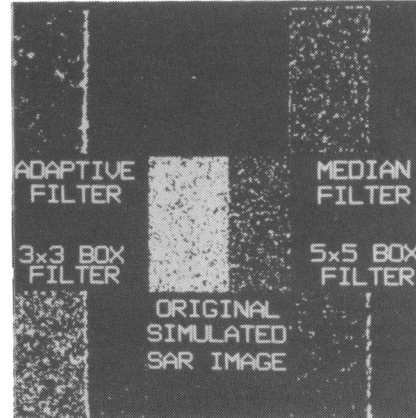
Processing Algorithm	S/N=1			S/N=14.6		
	3dB	6dB	9dB	3dB	6dB	9dB
Original	6.0	5.5	6.4	6.3	6.2	7.0
Median	6.8	6.2	8.4	7.1	11.3	17.8
3x3	9.5	7.8	13.2	9.1	14.4	17.8
5x5	8.2	13.0	15.3	23.3	52.9	67.7
Adaptive	9.2	11.9	17.3	43.2	56.4	62.6



(a)



(b)



(c)

Fig. 5. Edge experiment results for 6 dB edge height with $S/N = 14.6$.
(a) Input images. (b) Robert's gradient images. (c) Edge maps.

there is no benefit for edge detection. This is a direct result of the bandpass nature of radar images [36], [37]. The resulting edge maps for each processing scheme for this case are presented in Fig. 5(c).

In summary, an experiment has been conducted to quantitatively evaluate the adaptive filter as applied to SAR imagery. Four other processing algorithms were also evaluated as a basis for comparison. The edge map quality was used as the performance criterion. The adaptive filter provided better edge maps than the 3×3 box and median operators for both the $S/N = 1$ and $S/N = 14.6$ cases. The 5×5 box filter generated edge maps of similar quality to the adaptive filter except for low contrast edges. However, when resolution is also considered the adaptive filter is considered to be the best processing algorithm of those used in this study.

VI. CONCLUSIONS

A system model for imaging radars was developed and the model was used to design an adaptive filter algorithm to smooth noisy radar images. It was shown that the radar image is corrupted by multiplicative noise due to fading. The multiplicative model was used to derive the functional form of an optimum filter for enhancement of radar images. An adaptive version of the filter was designed and its performance was evaluated both quantitatively and qualitatively using simulated and actual radar images.

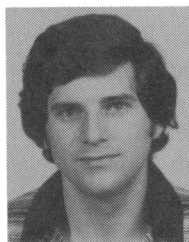
The filter presented in this paper is easily implemented in the spatial domain and is computationally very efficient. In addition to its use for smoothing noisy radar images, the filter can also be used for processing other images that are degraded

by a multiplicative noise process. For example, the degradation due to illumination changes in an optically produced image can be removed using a similar adaptive filter. The problems associated with digital radar image processing have just begun to be addressed. The radar system model presented here can be used for deriving feature extraction and classification schemes for analyzing the contents of radar images. The edge quality experiment clearly indicates a need for the development of specialized edge detection algorithms for radar. Other optimization criteria for the filter design should be considered. For example, criteria more closely related to specific applications, either human interpretation [40] or machine analysis, should be used in the development of advanced processing algorithms.

With the increasing availability of digital radar imagery, digital image processing techniques will be called upon to improve both the quantity and quality of the extracted information. Techniques which incorporate the unique characteristics of radar imagery, like the one presented here, can be used to derive the optimum processing algorithm for a given application.

REFERENCES

- [1] T. F. Bush and F. T. Ulaby, "Fading characteristics of panchromatic radar backscatter from selected agricultural targets," *IEEE Trans. Geosci. Electron.*, vol. GE-13, pp. 149-157, Oct. 1976.
- [2] J. W. Goodman, "Some fundamental properties of speckle," *J. Opt. Soc. Amer.*, vol. 66, pp. 1145-1150, Nov. 1976.
- [3] —, "Noise in coherent optical processing," in *Optical Information Processing*. New York: Plenum, 1976.
- [4] J. C. Holtzman, V. S. Frost, J. A. Stiles, and V. H. Kaupp, "Radar image simulation," *IEEE Trans. Geosci. Electron.*, vol. GE-16, pp. 296-303, Oct. 1978.
- [5] A. V. Oppenheim, R. W. Schafer, and T. G. Stockham, "Nonlinear filtering of multiplied and convolved signals," *Proc. IEEE*, vol. 56, no. 8, 1968.
- [6] R. O. Harger, *Synthetic Aperture Radar Systems*. New York: Academic, 1970.
- [7] J. R. Bennett and I. G. Cumming, "A digital processor for the production of Seasat synthetic aperture radar imagery," in *Proc. SURGE Workshop*, ESRIN, Frascati, Italy, July 1979, ESA Reprint SP-154.
- [8] E. J. Kovaly, *Synthetic Aperture Radar*. Dedham, MA: Artech House, 1976.
- [9] W. B. Davenport and W. L. Root, *Random Signals and Noise*. New York: McGraw-Hill, 1958.
- [10] J. W. Goodman, *Introduction to Fourier Optics*. New York: McGraw-Hill, 1968.
- [11] W. A. Penn, "Signal fidelity in radar processing," *IRE Trans. Mil. Electron.*, vol. MIL-6, pp. 204-218, Apr. 1962.
- [12] L. J. Porcello, "Speckle reduction in synthetic-aperture radars," *J. Opt. Soc. Amer.*, vol. 66, no. 11, pp. 1305-1311, 1976.
- [13] J. S. Zelenka, "Comparison of continuous and discrete mixed-integrator processors," *J. Opt. Soc. Amer.*, vol. 66, no. 11, pp. 1295-1304, 1976.
- [14] R. K. Moore, "Trade-off between picture element dimensions and noncoherent averaging in sidelooking airborne radar," *IEEE Trans. Aerosp. Electron. Syst.*, vol. AES-15, pp. 697-708, Sept. 1979.
- [15] G. R. Dicaprio and J. E. Wasielewski, "Radar, image processing, and interpreter performance," *Photogrammetr. Eng. and Remote Sensing*, vol. 52, pp. 1043-1048, Aug. 1976.
- [16] J. C. Dainty, *Laser Speckle and Related Phenomena*. New York: Springer, 1975.
- [17] P. Hariharan and Z. S. Hegedus, "Reduction of speckle in coherent imaging by spatial frequency sampling, Part II," *Opt. Acta*, vol. 21, no. 9, 1974.
- [18] W. K. Pratt, *Digital Image Processing*. New York: Wiley, 1978.
- [19] H. C. Andrews and B. R. Hunt, *Digital Image Restoration*. Englewood Cliffs, NJ: Prentice-Hall, 1977.
- [20] K. R. Castleman, *Digital Image Processing*. Englewood Cliffs, NJ: Prentice-Hall, 1979.
- [21] J. F. Walkup and R. C. Choens, "Image processing in signal dependent noise," *Opt. Eng.*, vol. 13, pp. 250-266, May/June 1974.
- [22] K. Kondo, Y. Ichioka, and T. Suzuki, "Image restoration by Wiener filtering in the presence of signal dependent noise," *Appl. Opt.*, vol. 16, Sept. 1977.
- [23] F. Naderi and A. A. Sawchuk, "Detection of low-contrast images in film-grain noise," *Appl. Opt.*, vol. 17, pp. 2883-2891, Sept. 15, 1978.
- [24] C. H. Chen, "Adaptive image filtering," in *Proc. Pattern Recog. and Image Processing Conf.*, Chicago, IL, Aug. 1979, pp. 32-37.
- [25] D. P. Panda, "Nonlinear smoothing of picture," *Comput. Graphics and Image Processing*, vol. 8, pp. 259-270, Aug. 1978.
- [26] J. S. Lee, "Digital image enhancement and noise filtering by use of local statistics," *IEEE Trans. Pattern Anal. Machine Intell.*, vol. PAMI-2, pp. 165-168, Mar. 1980.
- [27] D. P. Meyer and H. A. Mayer, *Radar Target Detection*. New York: Academic, 1973.
- [28] V. S. Frost, "Development of statistical models for radar image analysis and simulation," M.S. thesis, Univ. of Kansas, Lawrence, 1978.
- [29] R. K. Moore, "Microwave remote sensors," in *Remote Sensing Manual*, R. G. Reeves, Ed. Falls Church, VA: Amer. Soc. of Photogrammetry, 1975, ch. 9.
- [30] L. E. Franks, *Signal Theory*. Englewood Cliffs, NJ: Prentice-Hall, 1969.
- [31] A. Habibi, "Two-dimensional Bayesian estimation of images," *Proc. IEEE*, vol. 60, pp. 878-884, July 1972.
- [32] V. S. Frost, J. A. Stiles, and J. C. Holtzman, "Radar image processing," Remote Sensing Lab., Univ. of Kansas, Lawrence, Tech. Rep. TR 420-1, Jan. 1980.
- [33] A. D. Goldfinger, "SEASAT SAR processor signatures: Point targets," JHU/APL Tech. Rep. CP 078, Apr. 1980.
- [34] I. E. Abdou and W. K. Pratt, "Quantitative design and evaluation of enhancement/thresholding edge detectors," *Proc. IEEE*, vol. 67, no. 5, pp. 753-763, 1979.
- [35] F. M. Dicky, "Image oriented analysis of synthetic aperture radar systems," Ph.D. dissertation, Univ. of Kansas, Lawrence, 1974.
- [36] W. M. Brown and C. J. Palermo, *Random Process, Communication and Radar*. New York: McGraw-Hill, 1969.
- [37] R. N. Bracewell, *The Fourier Transform and Its Applications*, 2nd ed. New York: McGraw-Hill, 1978.
- [38] R. E. Morden and R. L. Withman, "An analysis of SAPPHIRE image parameters as a function of processing parameters," in *Proc. NAECON 1979*, vol. 2, 1979, pp. 818-824.
- [39] W. A. Pearlman, "A visual system model and a new distortion measure in the context of image processing," *J. Opt. Soc. Amer.*, vol. 68, pp. 374-386, Mar. 1978.
- [40] M. Perry, "Correlation analysis of SEASAT-SAR in the Southern Appalachians," M.S. thesis, Dep. Geology, Univ. of Kansas, Lawrence, Dec. 1980.



Victor S. Frost (S'75) was born in Kansas City, MO, on March 6, 1954. He received the B.S. and M.S. degrees in electrical engineering from the University of Kansas, Lawrence, in 1977 and 1978, respectively.

From 1974 to 1977 he was a Research Technician at the University of Kansas Remote Sensing Laboratory (RSL). From 1977 to 1978 he was a Research Engineer at RSL engaged in radar simulation and modeling research with emphasis on imaging systems. Currently, he is a Project Engineer at RSL pursuing the Ph.D. degree in electrical engineering, with research interests in stochastic modeling and digital processing of radar images.

Mr. Frost has received an Honors Undergraduate Research Grant from the University of Kansas. He was a Student Branch Chairman of the IEEE at the University of Kansas. He is a member of Eta Kappa Nu and Tau Beta Pi.

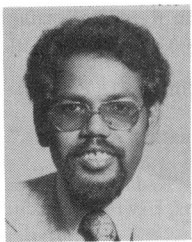


Josephine Abbott Stiles (S'75) was born in Lyons, KS, on March 12, 1952. She received the B.S. degree in engineering physics in 1974 and the M.S. degree in electrical engineering in 1977, both from the University of Kansas, Lawrence.

In 1976 she joined the Remote Sensing Laboratory of the University of Kansas, Lawrence, as a Research Assistant, at which time she was involved in the design and testing of small antennas for mobile traffic control. Recently, she

has been engaged in radar simulation research for the purposes of both image analysis and radar guidance. At present, she is a Research Engineer at the Remote Sensing Laboratory and is working toward the Ph.D. degree in electrical engineering.

Mrs. Stiles has been a Student Branch President of IEEE at the University of Kansas and has been actively involved in a number of university service organizations. She is a member of Eta Kappa Nu.



K. S. Shanmugan (M'70-SM'75) was born in India on January 6, 1943. He received the B.E. degree from Madras University, Madras, India, in 1964, the M.E. degree from the Indian Institute of Science, Bangalore, India, in 1966, and the Ph.D. degree from Oklahoma State University, Stillwater, in 1970, all in electrical engineering.

From 1970 to 1973 he worked as a Post-Doctoral Fellow at Oklahoma State University and the University of Kansas Center for Research, where he worked on problems in pattern recognition, image processing, and modeling and analysis of communication systems. From 1973 to 1978 he was with the Department of Electrical Engineering at

Wichita State University, Wichita, KS, where he taught and conducted research in systems theory, communication systems, and image processing. From December 1978 to January 1980 he was a Visiting Scientist at Bell Laboratories, Holmdel, NJ, where he worked on problems in the modeling and analysis of satellite communication systems. He joined the University of Kansas, Lawrence, in January 1980 as an Associate Professor of Electrical Engineering. His current interests are in the area of image processing and communication theory. He has published a number of articles in the above areas and is the author of a textbook, *Digital and Analog Communication Systems* (New York: Wiley, 1979).

Dr. Shanmugan is a member of the American Society for Engineering Education and the Society for Automotive Engineers (SAE). He received the Outstanding Young Engineering Faculty Award from SAE in 1979.



Julian C. Holtzman (S'63-M'66) was born in Staten Island, NY, on August 14, 1935. He received the B.S.E.E. degree from the Polytechnic Institute of New York, Brooklyn, NY, in 1958, the M.S. degree from the University of California, Los Angeles, in 1962, and the Ph.D. degree from Cornell University, Ithaca, NY, in 1967.

From 1958 to 1962 he worked for the Hughes Aircraft Company in the areas of radar, antennas, and communications satellites; he also served as a Consultant to Lockheed Missiles and Space Company and Applied Technology. After teaching at San Jose State University, San Jose, CA, from 1965 to 1969, he joined the faculty of the University of Kansas, Lawrence, where he presently is a Professor, Staff Member of the Remote Sensing Laboratory, and Chairman of the Department of Electrical Engineering. His current fields of research encompass tele- and data communications, radar systems, simulation, image processing, and analysis.

Dr. Holtzman is a member of Eta Kappa Nu and Sigma Xi.